Elucidating the Mode of Action of a Corrosion Inhibitor for Iron

Marcus Frey,[a] Steven G. Harris,[b] Jeremy M. Holmes,[b] David A. Nation,[b] Simon Parsons,[b] Peter A. Tasker,*[b] and Richard E. P. Winpenny[b]

Abstract: Two polymetallic iron(III) complexes **1** and **2** have been synthesised from the known corrosion inhibitor 3-(4-methylbenzoyl)-propionic acid HL^1 and their crystal structures determined. Coordination geometries extracted from these structures have been used as the basis for molecular modelling onto idealised iron(III) oxide surfaces as an aid to understanding the efficacy of inhibitors of the 4-keto acid type. The proposed mode of action involves 1,3-bridging didentate coordination of the carboxylate function of L^1 to two Fe^{III} ions, hydrogen-bond formation between the 4-keto group of L^1 and a bridging surface hydroxy group, as well as close packing of the aromatic end groups, which should generate a hydrophobic barrier on the surface. Adsorption isotherm experiments have been used to compare the strengths of binding of related carboxylic acids onto iron(III) oxide surfaces and indicate that the presence of the 4-keto function leads to the formation of significantly more stable surface complexes.

Keywords: coordination modes · corrosion inhibition · iron · molecular modelling · polynuclear complexes

Introduction

The design of ligands to bind strongly to metal oxide surfaces is likely to involve very different criteria from those needed to ensure stable complex formation in solution. For the latter situation, a multidentate ligand (Scheme 1) which defines most or all of the coordination sites on a single metal ion in a strain-free, and preferably preorganised form of the ligand, will give high thermodynamic stability on both enthalpic and entropic grounds and thus lead to encapsulation of the metal ion. Such an approach cannot be used to design a good surface ligand because many of the coordination sites of surface metal ions are imbedded in the oxide substructure. To enhance the strength of binding in such a system it will be beneficial to use a sufficiently rigid multidentate, polynucleating ligand that will address as many metal ions as possible in the surface array but not lead to sequestration of the metal into solution. Formation of such a polynuclear complex with an unstrained form of the ligand will be associated with favourable free energy terms similar to those of the chelate or macrocyclic effect.[1]

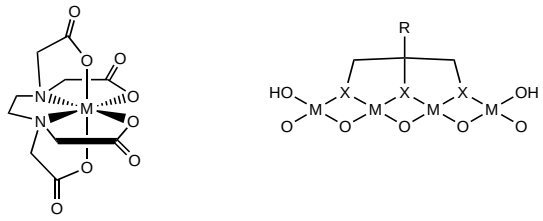

Scheme 1. Diagram showing the difference between a ligand designed to address one metal ion (sequestering) or several metal ions in a surface array (polynucleating).

Modification of surface properties to generate a range of useful effects has been approached[2] by functionalising the polynucleating ligand. Whilst such an approach has been demonstrably effective in "surface engineering", there have been few studies to define the nature of complexes formed at the metal(oxide) surfaces. Herein we consider the mode of action of a known corrosion inhibitor for iron and a range of structurally related molecules in an attempt to establish whether efficacy can be related to complex formation at the oxidised metal surface.

The protection of metal surfaces against wear and corrosion is an important area of industrial application.[3] In the case of steel, metallic pretreatments incorporating chromium(VI)[4] and other metals[5] have proved effective in reducing the activity of the surfaces. However, the potential carcinogenic and ecotoxic hazards posed by solutions of chromium(VI) employed in the manufacturing process have led to a greater

[a] Dr. M. Frey
Ciba Specialty Chemicals Inc.
4002 Basel (Switzerland)

[b] Prof. P. A. Tasker, Dr. S. G. Harris, Dr. J. M. Holmes, Dr. D. A. Nation, Dr. S. Parsons, Dr. R. E. P. Winpenny
Edinburgh Centre for Surface Coordination Chemistry
Department of Chemistry, The University of Edinburgh
West Mains Road, Edinburgh EH9 3JJ (UK)
Fax: (+44) 131-650-6452
E-mail: p.a.tasker@ed.ac.uk

  0947-6539/00/0608-1407 $ 17.50+.50/0

impetus for their replacement by more benign substances.[6, 7] Surface treatments based on organic ligands have demonstrated a range of desired effects including adhesion promotion, corrosion resistance, antiwear and mould-release properties.[2] Therefore, by suitable design, a particular organic ligand should be able to supply the desired surface effect without the ecological risk associated with heavy metal treatments. The corrosion inhibitor for iron, 3-(4-methylbenzoyl)-propionic acid, HL^1 (Scheme 2), produced by Ciba

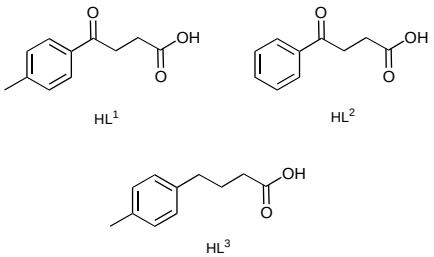

Scheme 2. Structures of the ligands HL^1, HL^2 and HL^3.

Specialty Chemicals for use in water-borne coatings, meets this criterion. Testing of this compound and the related derivatives HL^2 and HL^3 has shown[8] that the presence of both the methyl group in the *para* position of the aromatic ring and the carbonyl group gives rise to a greater effectiveness as a corrosion inhibitor in protective coatings. An understanding of the mode of action of such an inhibitor on the iron oxide surface will facilitate the design of more effective anticorrosion agents. In practice, obtaining such an understanding under the conditions of use of the corrosion inhibitor is an extremely difficult task. Most surface-analytical techniques give a wealth of information concerning composition, but few can supply details of surface structure, and hence of the binding mode of the ligand to the metal. This information, and in particular a knowledge of the types and structures of complexes formed at the metal(oxide) surface, will be needed for rational design of surface ligands. In order to acquire this information, use can be made of the tools available to the inorganic chemist, such as the preparation of metal complexes and their study by single-crystal X-ray diffraction. In a preliminary communication[9] we described an approach to this complex problem based on the synthesis and structural characterisation of polynuclear iron(III) complexes of known corrosion inhibitors (for example, HL^1) and the use of the defined structural motifs to model potential binding sites on iron(III) oxide surfaces. We now report fully our earlier work and present further evidence in the form of adsorption isotherm studies that support our model for the mode of action of HL^1.

Results and Discussion

Synthesis and structures: Central to the understanding of how ligands may bind to metal oxide surfaces is knowledge of their metal coordination chemistry. X-ray structure determinations of polynuclear complexes formed from solution can provide an understanding of how the ligands address the coordination requirements of the metal. Relating these requirements to the situation of addressing an array of metal ions in an oxide surface can provide insight into how ligands such as HL^1 achieve their remarkable surface-protective qualities. To this end we have prepared and characterised a number of polynuclear iron(III) complexes of HL^1. Two of relevance to this work are described below. The synthesis of these complexes is based on methods previously reported[10, 11] by Lippard and co-workers.

Reaction of hydrated iron(III) nitrate with one equivalent of $Na(L^1)$ and two equivalents of sodium methoxide in methanol gave a yellow powder that was analysed to be $Fe(L^1)(OCH_3)_2$. Slow diffusion of methanol into a solution of this powder in DMF yielded yellow needles that were suitable for X-ray single-crystal diffraction. Structure solution and refinement showed the complex to be a decanuclear "ferric wheel" of formula $[Fe(OCH_3)_2(L^1)]_{10}$ (**1**) (Figure 1). The structure consists of a centrosymmetric ring of ten iron(III) atoms held together by twenty μ_2-methoxide ligands and ten 1,3-bridging carboxylate ligands. Each iron(III) atom is surrounded by six oxygen donors in a slightly distorted octahedral geometry.

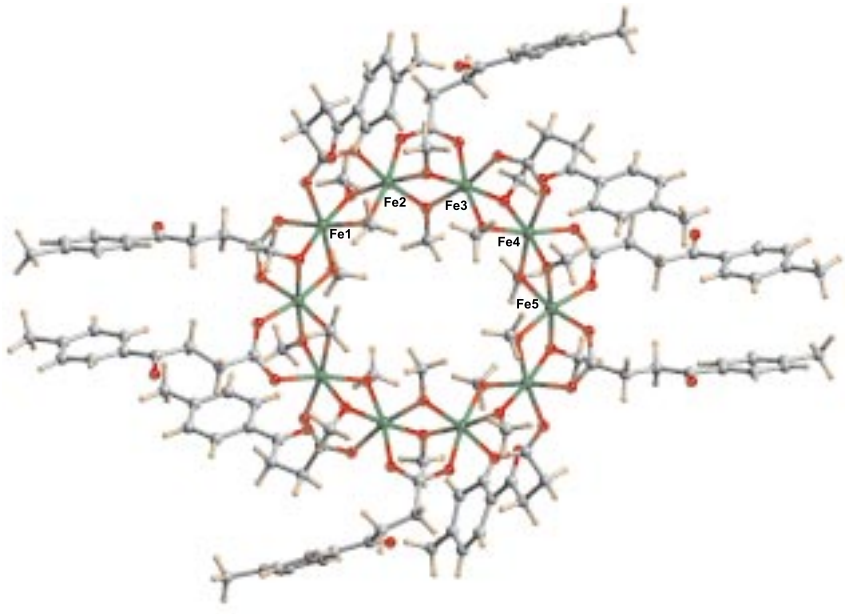

Figure 1. The structure of **1** in the crystal, showing the bonding of the carboxylate head-group to the Fe centres, and the non-involvement of the ketone function of L^1. (Fe: green; O: red; C: grey; H: light brown. These colours are also used in Figures 2, 4, 7, 8, 9, and 10.) Bond length ranges [Å]: Fe–O(methoxide) 1.962 – 2.000, Fe–O(L^1) 2.004 – 2.064 (esd 0.012). Bond angle ranges [°]: *cis* at Fe, 77.3 – 99.9; *trans* at Fe, 168.0 – 175.5 (esd 0.5).

0947-6539/00/0608-1408 $ 17.50+.50/0 *Chem. Eur. J.* **2000**, *6*, No. 8

The iron–oxygen bond lengths are typical and, except for its aesthetic appeal, the structure is unremarkable because similar decanuclear iron(III) wheels have been reported with both chloroacetate[10] and acetate[12] ligands in preparations that also used methanol as the solvent. In this work we found that to prepare polynuclear complexes other than **1**, the use of methanol in all stages of complex preparation and purification had to be avoided. In contrast to the ligands employed in these earlier reports, L^1 has the possibility of further interaction with the iron(III) centres through the carbonyl oxygen of the keto function, but, in the case of **1**, this potential is not realised and the ligand is merely dinucleating, spanning the apical sites of two edge-shared pseudo-octahedral iron(III) atoms.

The function of the keto carbonyl group of HL^1, in its role as a corrosion inhibitor, was hinted at from the structural determination of a second complex formed between iron(III) and L^1. Treatment of a solution of $Na(L^1)$ in water with an aqueous solution of iron(III) nitrate (0.43 equivalents) afforded a light orange powder. The material was analysed as the trinuclear species $[Fe_3(O)(L^1)_6(H_2O)_3] \cdot L^1$ and its identity was supported by FAB mass spectrometric measurements. Several oxo-centred trinuclear iron(III) complexes have been reported in the literature with carboxylate[13] and other ligands[14] and many have been crystallised.[15] Diffusion of diethyl ether vapour into a solution of the orange powder in acetonitrile afforded orange–brown crystals in very low yield which were suitable for X-ray diffraction. Structure determination and refinement indicated that hydrolytic oligomerisation of the oxo-centred trimer had occurred, resulting in an undecanuclear cage of formula $[Fe_{11}(O)_6(OH)_6(L^1)_{15}]$ (**2**) (Figure 2). Oligomerisations of this nature have been described in the literature. The formation of a similar undecanuclear iron(III) cage containing benzoate ligands has been ascribed[11] to hydrolytic oligomerisation of dinuclear $\{Fe_2O\}^{4+}$ units, whilst the fusion of two of these undecanuclear iron(III) benzoate complexes into a heptadecanuclear complex has been suggested[16] to involve the loss of $\{Fe_3O\}^{7+}$ fragments.

The structure of **2** is more complex than that of **1** and can be described as a distorted trigonal prism (defined by Fe3, Fe4, Fe6, Fe7, Fe9 and Fe10) with two iron atoms (Fe1 and Fe2) capping the triangular faces and three iron atoms (Fe5, Fe8 and Fe11) capping the rectangular faces. Holding the metal cluster together are six μ_3-oxide ions lying within the polyhedron, and six μ_3-hydroxide ions lying on its surface diagonally spanning the square faces with –OH–Fe–OH– bridges. The μ_3-oxide ions bridge between one iron on a vertex, one capping a triangular face and one capping a square face (for example, Fe2, Fe9 and Fe11), whereas the μ_3-hydroxide ions bridge two metal atoms at the vertices and one capping a rectangular face (such as Fe9, Fe10 and Fe11). Completing the coordination requirements of the iron(III) ions are the carboxylate oxygen atoms of fifteen L^1 ligands that each span pairs of adjacent edge-sharing pseudo-octahedral iron atoms. The iron–oxygen(oxido) bond lengths are much shorter (av 1.909(17) Å) than the iron–oxygen(hydroxido) bond lengths (av 2.096(40) Å), which allows clear distinction between these two ligand types. In complex **2**, as in **1**, L^1 binds to adjacent iron(III) atoms through its carboxylate function in a 1,3-bridging mode. Although the 3-keto oxygen atoms of L^1 ligands are not coordinated to metal ions in **2**, they act as hydrogen-bond acceptors for four of the six μ_3-hydroxide ions on the surface of the iron(III)–oxo cluster (Figure 2). The reason why two of the six bridging hydroxide ions are not involved in a similar interaction with a nearby L^1 ligand is unclear; they are however hydrogen-bonded to solvent (not shown).

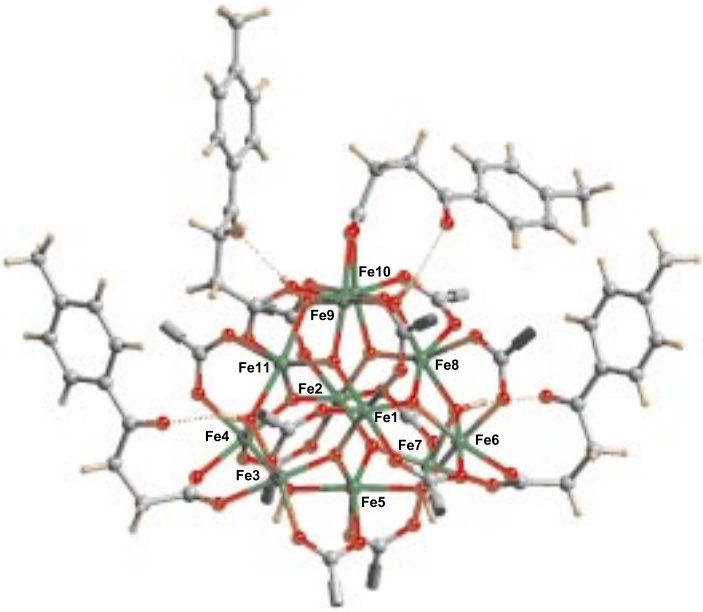

Figure 2. The structure of **2** in the crystal, viewed along the pseudo-trigonal axis of the metal polyhedron. The organic tail group of eleven of the L^1 ligands is excluded for clarity. The four L^1 ligands depicted have hydrogen bonds, shown as dotted lines, to hydroxides bridging the metal core. Bond length ranges [Å]: Fe–O(oxide) 1.878–1.941, Fe–O(hydroxide) 2.049–2.176, Fe–O(L^1) 1.936–2.158 (esd 0.008). Bond angle ranges [°]: *cis* at Fe, 75.9–109.3; *trans* at Fe, 154.6–177.4 (esd 0.3).

The change in stretching frequency of the carbonyl group of L^1 upon hydrogen bonding to the bridging hydroxide of the metal cluster in **2** is clearly evident in the Raman spectrum (Figure 3). Four of the fifteen L^1 ligands in **2** are engaged in hydrogen bonding with the cluster, which results in an asymmetric doublet for the ν(C–O) vibrational mode. The frequency of vibration of the hydrogen-bonded carbonyl group would be expected to be lower than that of the non-interacting carbonyl groups, and this is evident in the spectrum. The higher frequency peak, located at 1685 cm^{-1} in **2**, matches closely that of the cyclic complex **1**, where the ten L^1 ligands are equivalent and a single peak for the carbonyl stretching vibration is expected, as well as the carbonyl vibration in the spectrum of uncomplexed HL^1 (1684 cm^{-1}).

Three of the four L^1 molecules that are hydrogen-bonded to the surface of the cluster have very similar geometries (Figure 4), and the associated $Fe_2(OH)L^1$ unit can be considered as a potential model for docking on to the surfaces of known iron(III) oxides (see below). The 1,3-bridging carboxylate group has a geometry similar to that in the non-hydrogen-bonded ligands and to that observed for L^1 in the decanuclear complex **1** (Table 1).

The combination of the conventional dinucleating mode of coordination of the carboxylate group with the secondary

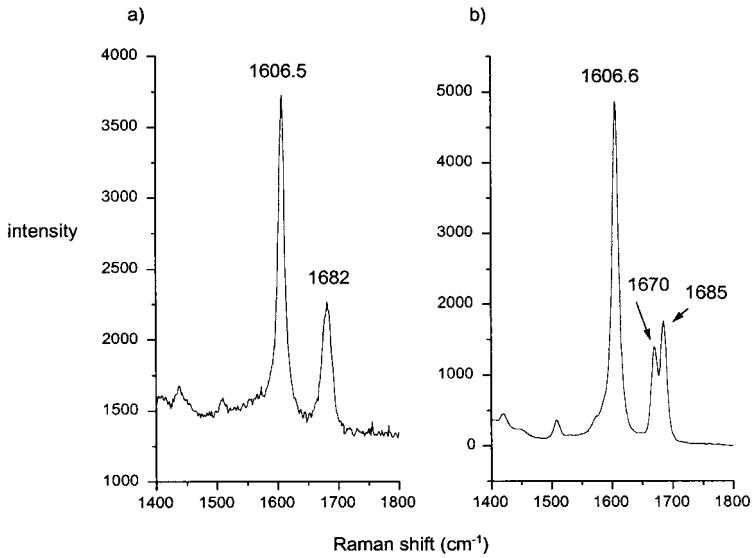

Figure 3. Raman spectra of a) complex **1** and b) complex **2**, showing the splitting of the carbonyl stretching frequency in the latter complex. The intensity axes have arbitrary units.

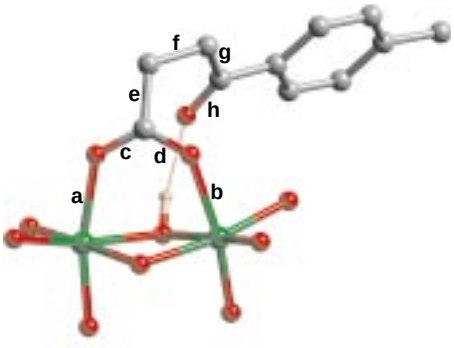

Figure 4. The conformation of the hydrogen-bonded ligand L^1 observed in complex **2** and in models for attachment to the (021) plane of lepidocrocite. (Hydrogen atoms of L^1 have been omitted for clarity.)

bonding of the 3-keto group in L^1 may provide a partial explanation for its efficacy as a corrosion inhibitor. Evidence that such a "multisite attachment" to iron(III) oxides leads to an increase in strength of binding beyond that for simple carboxylates was sought by carrying out adsorption isotherm measurements.

Adsorption isotherms: In order to investigate the effects of structural changes in HL^1 on its ability to bind to an iron oxide surface we have conducted solution adsorption isotherm experiments. The adsorbent chosen was a pigmentary iron(III) oxide purchased from Bayer AG. The oxide was identified by X-ray powder diffraction to be goethite (α-FeO(OH)). Solutions of HL^1, HL^2 and HL^3 in methanol/water (95:5 v/v), with concentrations in the range 6.0×10^{-5} to 3.0×10^{-3} mol L^{-1}, were allowed to equilibrate at 25 °C with known amounts of the oxide. Measurement of the concentration of the remaining ligand in solution by UV spectroscopy allowed the amount of ligand adsorbed onto the iron oxide surface to be calculated. Plots of amount adsorbed versus equilibrium concentration are given in Figure 5.

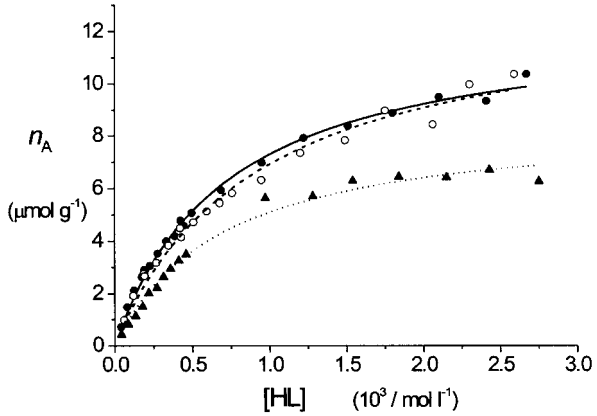

Figure 5. Adsorption isotherms for HL^1 (●, ——), HL^2 (○, - - - -) and HL^3 (▲, ••••). The lines through the data points represent best fits to the Langmuir adsorption equation.

Table 1. Selected bond lengths [Å] and torsion angles [°] for the ligand L^1 observed[a] in the three unique ligands with a similar *gauche* conformation at the methylene–methylene bond in complex **1**, in four hydrogen-bonded units in complex **2**, and in two models, **A** and **B**, for attachment to the (021) plane of lepidocrocite.

	Complex **1**	Complex **2[a]**	Complex **2[b]**	Complex **2[c]**	Complex **2[h]**	Model **A**	Model **B**
FeLFe [Å]	3.021(5)[b]	3.132(3)	3.160(3)	3.166(3)	3.015(3)	3.060	3.060
Fe–O [Å]	2.032(19)[b]	2.048(9)	2.050(8)	2.068(8)	2.069(8)	2.015	2.072
Fe–O [Å]	2.032(19)[b]	2.005(9)	2.013(8)	2.009(8)	2.010(8)	2.015	1.935
(C=)OLO [Å]	N/A	2.870(12)	2.879(12)	2.908(12)	3.233(12)	2.929	2.86(3)[d]
C=OLO(H) [°]	N/A	124.4(10)	129.4(10)	126.3(10)	137.5(10)	129.7	143(3)[d]
ace [°]	184(3)[c]	156.0(19)	158.1(8)	158.9(9)	151.4(9)	166.7	177.6
bde [°]	−183(3)[c]	−151.5(8)	−146.8(9)	−149.9(9)	−162.6(8)	−166.9	−175.6
cef [°]	−161(5)[c]	−135.9(12)	−139.2(12)	−140.9(12)	−148.0(12)	−115.9	−6.7
def [°]	26(8)[c]	45.4(15)	37.2(16)	38.2(16)	30.9(17)	59.7	175.6
efg [°]	67(4)[c]	58.0(15)	57.7(15)	53.7(16)	52.4(17)	49.4	71.6
fgh [°]	0(8)[c]	−3.8(19)	−1.5(17)	4.8(19)	−1.6(21)	−8.7	−17.6

[a] The labelling scheme for bonds is shown in Figure 4. [b] Average values with their associated standard deviations, *s*, for the five crystallographically unique ligands. [c] Average values with their associated standard deviations, *s*, for the three unique ligands with *gauche* conformations at **efg**. [d] Average values for three trifurcated hydrogen bonds.

0947-6539/00/0608-1410 $ 17.50+.50/0 *Chem. Eur. J.* **2000**, *6*, No. 8

The data for each ligand can be fitted satisfactorily to a Langmuir adsorption model [Eq. (1)], where θ is the fraction

$$\theta = \frac{K[\mathrm{HL}]}{(1 + K[\mathrm{HL}])} \text{ and } \theta = \frac{n_A}{n_M} \quad (1)$$

of surface sites occupied, that is, the measured amount of ligand (n_A) adsorbed on the oxide surface divided by the theoretical amount of ligand (n_M) needed to provide monolayer coverage, and K is the equilibrium adsorption constant. The results of curve fitting to this model are given in Table 2 and, along with the raw data, are shown in Figure 5. The differences between equilibrium adsorption constants (K) for the ligands, as determined by the fitting procedure (Table 2), do not appear to be significant whereas examination of

Table 2. Adsorption isotherm constants (standard deviations in parentheses).

	HL^1	HL^2	HL^3
$n_M\ 10^5$ [mol g^{-1}]	1.26(2)	1.32(5)	0.87(4)
$K\ 10^{-3}$ [L mol^{-1}]	1.4(1)	1.1(1)	1.4(1)

Figure 5 clearly reveals that the ligands do exhibit different binding strengths. The numerical fits have been performed for all the data points, some of which, it could be argued, should be discarded as being outside the expected limits of experimental error. For this reason a qualitative description only of binding strengths will be given, which is based on comparison of the slopes of the essentially linear portions of the curves that are to be found at low equilibrium concentrations (less than 5×10^{-4} mol L^{-1}). In this region surface coverage is low and binding strength is proportional to the slope of the isotherm. In this regard therefore it can be seen that HL^1 and HL^2 follow essentially the same isotherm and have similar slopes in the concentration region 0 to 5×10^{-4} mol L^{-1}, whereas HL^3 behaves quite differently and has a lesser slope in the low concentration region. This indicates that HL^1 and HL^2 have similar adsorption binding strengths that are both greater than that of HL^3. In view of the structural differences between the three ligands the presence of the keto function in HL^1 and HL^2 must be the cause of the enhanced binding that is observed with the iron oxide surface over that achieved by HL^3. We suggest that this could be a result of a favourable hydrogen-bonding interaction between the keto oxygen and a terminal hydroxide group on the oxide surface.

Despite the clear distinction between hydrogen-bonded and non-hydrogen-bonded carbonyl groups in the Raman spectra of **1** and **2** (Figure 3) attempts to probe the interaction of HL^1 and HL^2 directly on the oxide surface by both SERRS and DRIFT spectroscopy have to date been inconclusive. In other work,[17] DRIFT spectroscopy has been used to demonstrate the 1,3-bridging mode of coordination of a carboxylate ligand to the surface of goethite.

Within experimental error there is no difference between the fitted curves for HL^1 and HL^2. This suggests that the presence or absence of the *p*-methyl substituent in the aromatic ring has little or no influence on the adsorption of the ligands onto this oxide. Such a structural difference between HL^1 and HL^2 would certainly be expected to become important at higher concentration where steric effects between molecules packing on the surface need to be considered. For this particular batch of oxide the specific surface area has been determined by BET methods to be 18.8 m^2 g^{-1}. If we assume that monolayer coverage is occurring and we take into account the value of n_M determined from the fitted Langmuir equation (1.26×10^{-5} mol g^{-1}), we can calculate the surface area on the oxide occupied by a single molecule of HL^1 to be 248 Å^2. This is approximately five times larger than the theoretical amount calculated for a single molecule of HL^1 bound to an idealised oxide surface (see below) and may therefore reflect a low density of suitable binding sites per unit area on the real oxide. With such a large area available to each individual HL^1 or HL^2 molecule the effects of steric interactions between adjacent ligands are unlikely to be observed in this experiment.

The efficacy of HL^1 in protective coatings is adversely affected by the presence of inorganic anions such as sulfate, chloride and perchlorate. At pH values below the point of zero charge, pH_{pzc}, (8.1 for goethite[18]) the oxide surface will carry a net positive charge and inorganic anions will be attracted to the surface where they are able to compete with the organic inhibitors for binding sites. Isotherm measurements have been used to investigate the competition between these anions and HL^1 for surface sites on goethite (Figure 6). In the presence of perchlorate (0.01 mol L^{-1}) the adsorption of

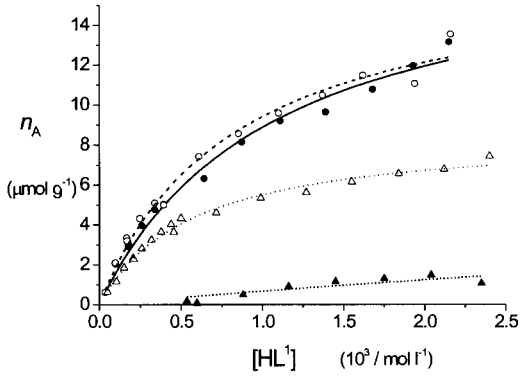

Figure 6. Adsorption isotherms for HL^1 alone (●, ——) and in the presence of 0.01 mol L^{-1} perchlorate (○, ----), chloride (△, ••••) and sulfate (▲, ••••).

HL^1 onto goethite does not seem to be affected and the isotherms for both HL^1 alone and with added perchlorate are identical within experimental error. The presence of chloride (0.01 mol L^{-1}) however causes the adsorption of HL^1 to be significantly reduced, which indicates that chloride is able to block some of the binding sites on the oxide surface. The effect of sulfate is even more dramatic with HL^1 only able to provide a fraction of its original surface coverage. This observed order of $SO_4^{2-} > Cl^- > ClO_4^-$ as competitors for displacement of L^1 agrees with that expected on the grounds of stability constants[19] of Fe^{III}–anion complexes with perchlorate either being non-coordinating or at best forming a very weak complex. The greater effectiveness of sulfate over chloride may be aided by the ability of sulfate ion to coordinate to goethite surfaces in a dinuclear bridging

mode[20] thus offering a thermodynamically more stable surface complex. The order of effectiveness of these inorganic anions as competitors for surface binding agrees with that found for promotion of corrosion by electrochemical measurements,[21] illustrating the importance of adsorption phenomena in the protection of metals.

Molecular modelling: An explanation of structure – activity relationships for the carboxylate ligands $L^1 - L^3$ and evidence for the "multisite attachment" to iron(III) oxide surfaces was sought from molecular modelling. The first step was to compare different iron oxide surfaces and select one for detailed study. It has been shown that the predominant oxide formed on lightly corroded iron surfaces is lepidocrocite (γ-FeO(OH)).[22] Bravais – Friedel – Donnay – Harker theory predicts[23] that the {020}, {021} and {110} Miller planes are responsible for 94 % of the total surface area of lepidocrocite. Layers coplanar with the (021) plane of lepidocrocite contain iron(III) and hydroxide ions in a very similar disposition to that found in **2**, namely edge-shared Fe^{III} octahedra, and for this reason this particular surface orientation was chosen initially as the model surface over the other two candidates. Depending on the conditions under which the iron has been corroded, magnetite and goethite may also be present in rust samples.[24] Very similar edge-shared Fe^{III} octahedra can be identified on the (001) plane of magnetite and the (110) plane of goethite.

The generation of the model surface requires cleavage of the lattice and breaking of Fe–O bonds. In order to satisfy the coordination requirements of the iron and oxide ions left exposed, the elements of water were added. For each hydroxy group that was terminally attached to a five-coordinate surface iron atom, a proton was attached to a surface μ_3-oxide.

We examined how dinuclear fragments from both **1** and **2**, consisting of L^1 with two iron(III) octahedra, could be mapped onto the generated surface in a periodic way to obtain the best overlap between the edge-shared octahedra of the fragment and those identified on the surface cell. One molecule of L^1 was attached to each (021) surface cell in an η^2 mode, displacing two terminal surface hydroxy groups. In reality this process would lead to a build-up of positive charge on the surface and would be compensated by a corresponding negative charge in the electric double layer.

The conformation of the ligand L^1 was allowed to change by energy minimisation with the Universal force field. The hydrogen-bonded L^1 in **2** has a *gauche* arrangement about the methylene – methylene bond with a torsion angle **efg** of about 60° (Figure 4). Such an arrangement should allow hydrogen-bond formation between the keto oxygen atom of L^1 and a bridging hydroxyl ligand in the (021) surface of lepidocrocite. For this reason the (C=)O···(H)O distance was restrained to 2.9 Å and the C=O···O angle was restrained to 130°. Resultant structural parameters are shown in Table 1 in the column headed "model **A**". These parameters are very similar to those found in the four hydrogen-bonded ligands in complex **2**. The energy minimised surface structure (model **A**) is shown in Figure 7.

While these modelling results confirm that L^1 can be attached to an iron(III) oxide surface by a combination of normal coordinate bonds to two iron centres and a hydrogen bond to surface hydroxide, they do not rule out other geometrical arrangements which can also give such "multisite attachment".

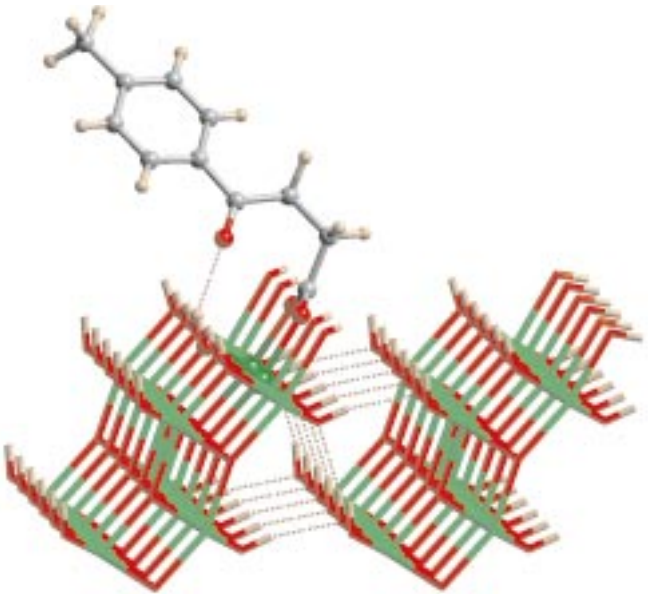

Figure 7. The bonding of a single molecule of L^1 to the 021 surface of lepidocrocite by the "multisite attachment" mode found in the complex **2**, with an intramolecular hydrogen bond in the dinuclear unit (model **A**). (Bond lengths and torsion angles in the complex are given in Table 1.)

An alternative mode of attachment is shown in model **B** (Figure 8). In this model the keto oxygen atom forms hydrogen bonds to hydroxyl units in adjacent rows of iron atoms. Because of the high density of hydroxyl groups on the surface, the keto group may be able to interact with several of these at once. In an energy minimisation similar to that described for model **A** but without any geometry restraints, the keto O atom simultaneously forms three (weak) contacts with surface hydroxy groups (O···O distances 3.06 Å, 3.30 Å, 3.40 Å).

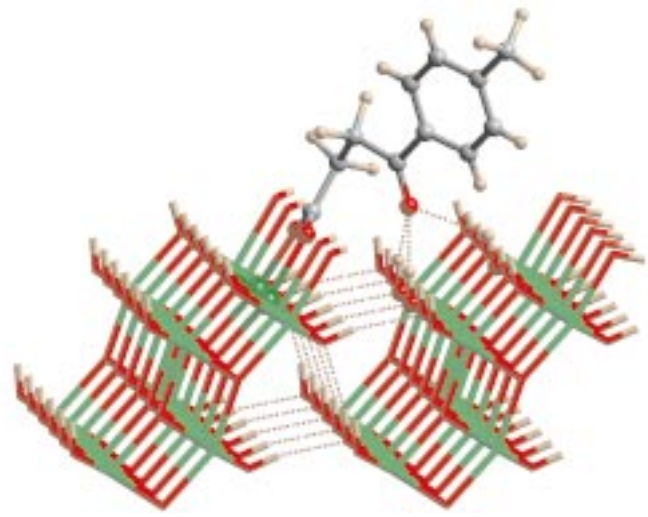

Figure 8. An alternative "multisite attachment" mode (model **B**) for bonding of a single molecule of L^1 to the (021) surface of lepidocrocite, involving hydrogen bonding to an array of hydroxy groups adjacent to the dinuclear unit. (Bond lengths and torsion angles in the complex are given in Table 1.)

0947-6539/00/0608-1412 $ 17.50+.50/0 *Chem. Eur. J.* **2000**, *6*, No. 8

When distance and angle restraints are applied as defined for model **A**, a viable trifurcating arrangement can be identified.

The geometrical parameters for the resultant model B are contained in Table 1. The major conformational difference between L^1 in models **A** and **B** is a rotation around bond **e** which joins the carboxylate and methylene groups. Respective values of torsions **cef** and **def** differ by approximately 110° in the two models. All other torsions lie within 10° of parameters observed in crystal structures. A *gauche* conformation is retained between methylene groups in each model. As in complex **2**, an X-ray structure determination of the free ligand HL^1 has shown this to adopt a *gauche* conformation between the methylene groups in the solid state (Figure 9). This implies that very little strain energy in the ligand will be involved in coordinating in either model **A** or **B**. It is also apparent that only minor conformational changes might be required to provide L^1 with the ability to interact with up to three hydrogen-bond donors at once.

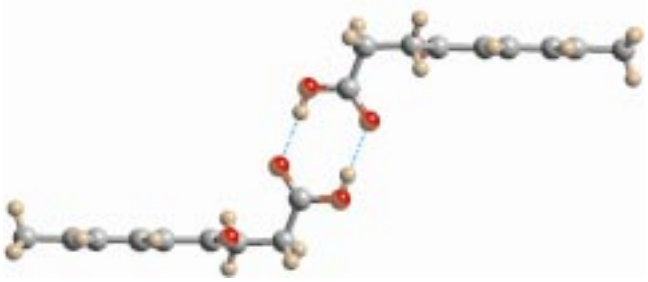

Figure 9. The dimeric structure of the free ligand HL^1 (aromatic rings viewed edge-on) showing the *gauche* conformation in the CH_2CH_2 unit.

The energy-minimised structures for models **A** and **B** have the aromatic ring lying at angles to the metal-oxide surface of 48° and 74°, respectively. Both of these periodic models have all of the surface binding sites occupied by L^1 ligands. Very good surface coverage is obtained with efficient packing (Figure 10). The area occupied by a single molecule is the same in both models and is equal to that of the surface cell, 45 Å^2. A very hydrophobic surface will result with very few gaps between the ligand molecules. This should provide a barrier to aggressive water-borne species such as oxygen and electrolytes, and hence provide an explanation for the efficacy as a corrosion inhibitor. The ligand HL^2 appears to bind equally strongly to iron(III) oxide surfaces according to the isotherm studies, but the lack of *para*-methyl substituent results in larger "holes" in the monomolecular surface film and hence could account for it being inferior[8] to HL^1 in protection of iron surfaces. Other types and positions of aromatic substitution make it difficult to retain both the bifunctional mode of attachment of the ligand to the surface as well as close packing of the aromatic end groups. Of course, the surface of corroded iron is not composed of just one face of one oxide, and modelling of HL^1 onto other candidates does not provide as good a surface coverage, but it just may be the case that the presence of HL^1, or indeed any surface active ligand, could influence the nature of the oxide surface that is formed in such a way as to favour its passivation. This has been demonstrated in a recent study on the hydrolysis and oxidation of iron(II), which has shown that the presence of sulfate salts leads to pure goethite, whereas chloride salts give a mixed product of goethite and lepidocrocite.[25]

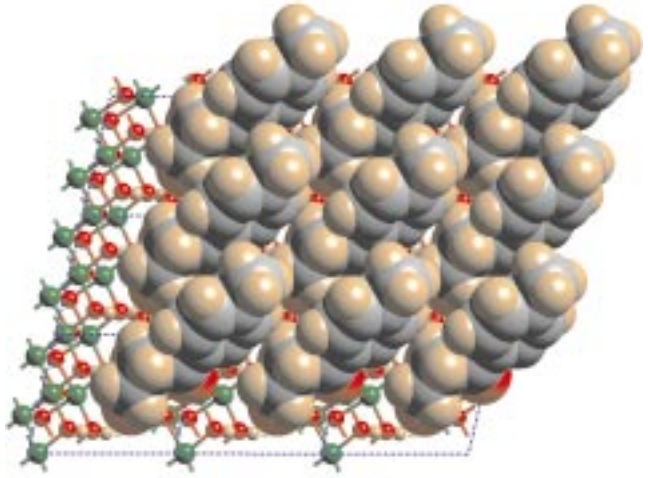

Figure 10. The packing of nine L^1 ligands on the (021) surface of lepidocrocite based on the bonding mode found in the structure of **2**. For each L^1 the carboxylate group is at the bottom left of the molecule as viewed, and the methyl group is at the top right.

It is perhaps particularly significant that the mode of application of HL^1 as the anticorrosive Irgacor 419 is in water-borne polymer coatings. The period involved in the curing and drying of these coatings will allow access of HL^1 to the iron oxide surface and permit reorganisation to form stable complexes of the types described above. An important feature of HL^1 is that it appears to be able to address different binding sites by the combination of the "classical" coordination bonds involved in dinuclear complex formation by carboxylates and secondary bonding of the 3-keto function to surface hydroxy groups.

These studies have drawn attention to the importance of ligand-to-surface hydrogen bonding as a method of enhancing the stability of surface complex formation. The design of ligands to exploit this and other forms of secondary bonding, including interligand interactions, is the subject of current work at Edinburgh.

Experimental Section

The ligands HL^1, HL^2 and HL^3 were supplied by Ciba Specialty Chemicals Inc., Basle, Switzerland. All other reagents were of analytical grade and were used as received.

Preparation of iron(III) complexes:

Complex 1: A solution of $Fe(NO_3)_3 \cdot 9H_2O$ (0.93 g, 2.3 mmol) in MeOH (10 mL) was added to a solution of $Na(L^1)$ (0.49 g, 2.3 mmol) in MeOH (20 mL). $NaOCH_3$ (5.0 mmol) in MeOH (5 mL) was added to the resulting orange-red solution, causing the precipitation of a yellow powder (0.60 g, 85 %) which was crystallised by the slow diffusion of MeOH into a solution in DMF to give a small quantity of yellow needles of $[Fe(OCH_3)_2(L^1)]_{10}$, **1**; $C_{130}H_{170}Fe_{10}O_{30}$: calcd: C 50.51, H 5.54; found: C 50.30, H 5.53.

Complex 2: A solution of $Fe(NO_3)_3 \cdot 9H_2O$ (3.23 g, 8.0 mmol) in H_2O (25 mL) was added to a solution of $Na(L^1)$ (4.01 g, 18.7 mmol) in H_2O (75 mL). The resulting light orange powder was collected, washed with H_2O, and dried under vacuum (3.83 g, 90 %). This material was identified as the trinuclear species $[Fe_3(O)(L^1)_6(H_2O)_3] \cdot L^1$; $C_{77}H_{83}Fe_3O_{25}$: calcd: C

Table 3. Crystallographic data for **1**, **2**, and HL^1.

	1 · MeOH	**2** · $C_4H_6O \cdot 3\,C_2H_3N \cdot 0.5\,H_2O$	HL^1
empirical formula	$C_{131}H_{174}Fe_{10}O_{51}$	$C_{175}H_{191}Fe_{11}N_3\ O_{58.5}$	$C_{11}H_{12}O_3$
M_w	3123.2	3886.7	192.21
space group	triclinic, $P\bar{1}$	triclinic, $P\bar{1}$	monoclinic, $P2_1/c$
a [Å]	10.537(4)	19.534(8)	5.837(1)
b [Å]	18.856(6)	21.320(11)	5.295(1)
c [Å]	19.392(7)	22.821(14)	31.613(9)
α [°]	101.23(2)	83.71(4)	90
β [°]	105.36(2)	74.13(4)	90.75(2)
γ [°]	94.96(2)	80.67(3)	90
V [Å^3]	3605(2)	9000(8)	976.8(4)
Z	1	2	4
T [K]	150.0(2)	220.0(2)	220.0(2)
crystal dimensions [mm]	$0.49 \times 0.16 \times 0.16$	$0.39 \times 0.27 \times 0.12$	$0.43 \times 0.23 \times 0.12$
$\mu(MoK_\alpha)$ [mm^{-1}]	1.06	0.94	0.095

58.68, H 5.31; found: C 59.69, H 5.23. Slow crystallisation by dissolution in MeCN and subsequent diffusion of diethyl ether into the solution produced a tiny amount of orange-brown crystals after several weeks (m.p. 165–167 °C). Characterisation by single-crystal X-ray diffraction identified the material as $[Fe_{11}(O)_6(OH)_6(L^1)_{15}]$, **2**.

Crystal structure determinations: Data for **1**, **2** and HL^1 were collected with a Stoe Stadi-4 diffractometer equipped with an Oxford Cryosystems low-temperature device (Table 3). Absorption corrections were applied with ψ scan data for **1** (min/max transmission for **1** = 0.455/0.585). All structures were solved by direct methods[26] and completed by iterative cycles of ΔF syntheses and full-matrix, least-squares refinement against F^2 (SHELXTL, Bruker AXS). Hydrogen atoms were included in the structures in calculated positions, riding on parent C atoms, with $U(H) = 1.2\,U_{eq}(C)$ for aromatic H atoms and $U(H) = 1.5\,U_{eq}(C)$ for methyl H atoms. For the structures of **1** and **2**, disordered and part-weight solvate molecules were found in the lattice which were modelled as MeOH in **1**, and as Et_2O, MeCN and H_2O in **2**. No solvent was present in the lattice of HL^1. All non-hydrogen atoms within the cages were refined with anisotropic displacement parameters: for **1**, 564 parameters, $wR2 = 0.3773$ for 9265 unique data ($2\theta \leq 45°$), $R1 = 0.1257$ for 3919 observed reflections with $F_o > 4\sigma(F)$, largest residual peak and hole were respectively 0.596 and -0.589 e Å^{-3}; for **2**, 2160 parameters, $wR2 = 0.2501$ for 19121 unique data ($2\theta \leq 42°$), $R1 = 0.0872$ for 10180 observed reflections with $F_o > 4\sigma(F)$, largest residual peak and hole were respectively 0.907 and -0.627 e Å^{-3}; for HL^1, 130 parameters, $wR2 = 0.1600$ for 1278 unique data ($2\theta \leq 45°$), $R1 = 0.0673$ for 555 observed reflections with $F_o > 4\sigma(F)$, largest residual peak and hole were respectively 0.156 and -0.206 e Å^{-3}. Crystallographic data (excluding structure factors) for the structures have been deposited with the Cambridge Crystallographic Data Centre as supplementary publication nos. CCDC-102414, 102415 and 134655 for **1**, **2** and HL^1, respectively. Copies of these data can be obtained free of charge on application to CCDC, 12 Union Road, Cambridge CB21EZ, UK (fax: (+44) 1223-336-033; e-mail: deposit@ccdc.cam.ac.uk).

Adsorption isotherm measurements: Preweighed quantities of goethite (0.40 g) in polycarbonate centrifuge tubes were stirred with the desired concentration of ligand in methanol/water (10 mL, 95:5 v/v) for 2 h at 25 °C. For studying the anion effects, tetrabutylammonium perchlorate, chloride, or hydrogensulfate was added to each tube in order to obtain a 0.01 mol L^{-1} solution of the anion. The suspensions were centrifuged and filtered, and the supernatant diluted if necessary, for absorbance measurement by UV spectrometry at 252, 242 and 213 nm for HL^1, HL^2 and HL^3, respectively (Unicam UV-2 spectrophotometer). The measured absorbance was related to the concentration of the ligand remaining in solution by reference to calibration curves. The amount of ligand adsorbed was then calculated from the difference between initial and final concentration. The data for each ligand were fitted to the Langmuir adsorption equation (see text) with Origin V5.0. The calculated equilibrium adsorption constants K and maximum amounts adsorbed (n_M) are given in Table 2.

Molecular modelling: All calculations were performed on a Silicon Graphics Indigo2 work-station equipped with the Cerius2 molecular modelling package from MSI. Bravais–Friedel–Donnay–Harker calculations predicted that for a single crystal of lepidocrocite the surface would comprise four sets of Miller planes: {020} (occupying 42.61 % of total surface area); {021} (29.04 %); {110} (22.83 %); {111} (5.52 %). No suitable carboxylate binding sites were found on the (020) plane, therefore calculations were carried for the (021) plane. The resulting surface cell had dimensions $u = 6.52$ Å, $v = 7.51$ Å, $\theta = 101.8°$. The ligand HL^1 was then attached to neighbouring ferric sites, with the result that the carbonyl group came into hydrogen-bonding proximity of a nearby μ_3-hydroxide. The surface structures were minimised with the Universal force field. This is not equipped with hydrogen-bond parameterisation so harmonic restraints were applied to treat those aspects of the structure. The tolyl group (with the exception of methyl H atoms) could be treated as a rigid body since crystal structure analyses showed this fragment to be planar. Positional and lattice parameters of the lepidocrocite were fixed. The retention of two-dimensional periodicity avoids so-called "edge effects", with an infinite number of surface cells implicitly inferred in both the u and v directions. The force field includes parameterisation for intermolecular contacts, so the energy minimisation procedure takes into consideration the surface packing arrangement. Resultant structural parameters are shown in Table 1.

Acknowledgements

We thank Ciba Specialty Chemicals and the EPSRC (UK) for a post-doctoral fellowship to D.A.N., the EPSRC (UK) for grants providing the diffractometer, the computer work-station and financial support (to S.G.H.), the Royal Society for an Industrial Fellowship (to J.M.H.) and Zeneca Specialities for financial support (to S.G.H.) and for providing software and assistance (Dr. R. Docherty) for molecular modelling. We also thank Prof. E. Smith and Dr. C. Rodger (Strathclyde University) for Raman spectra, Drs. G. McDougall and R. Brown for BET surface area determinations, and Gareth Oakley for powder XRD measurements.

[1] L. F. Lindoy, *The Chemistry of Macrocyclic Ligand Complexes*, Cambridge University Press, Cambridge, **1989**.
[2] M. Ellwood, S. W. Leeming, International Patent Application WO 95/19260, **1995**; J. M. Holmes, P. A. Tasker, European Patent EP400773, **1990**; J. R. Lawson, European Patent EP517356, **1992**; G. R. John, B. Tury, C. F. Walker, European Patent EP247728, **1987**.
[3] T. W. Swaddle, *Inorganic Chemistry: An Industrial and Environmental Perspective*, Academic Press, London, **1997**.
[4] M. Murase, J. F. Watts, *J. Mater. Chem.* **1998**, *8*, 1007.
[5] E. Almeida, T. C. Diamantino, M. O. Figueiredo, C. Sá, *Surf. Coat. Tech.* **1998**, *106*, 8.
[6] K. Doren, W. Freitag, D. Stoye, *Water-Borne Coatings: The Environmentally Friendly Alternative*, Hanser/Gardner, Cincinnati, **1994**.
[7] Yu. I. Kuznetsov, *Organic Inhibitors of Corrosion of Metals*, Plenum Press, New York, **1996**.
[8] Ciba Specialty Chemicals, unpublished work.

[9] M. Frey, S. G. Harris, J. M. Holmes, D. A. Nation, S. Parsons, P. A. Tasker, S. J. Teats, R. E. P. Winpenny, *Angew. Chem.* **1998**, *110*, 3435; *Angew. Chem. Int. Ed.* **1998**, *37*, 3246.
[10] K. L. Taft, C. D. Delfs, G. C. Papaefthymiou, S. Foner, D. Gatteschi, S. J. Lippard, *J. Am. Chem. Soc.* **1994**, *116*, 823.
[11] S. M. Gorun, G. C. Papaefthymiou, R. B. Frankel, S. J. Lippard, *J. Am. Chem. Soc.* **1987**, *109*, 3337.
[12] C. Benelli, S. Parsons, G. A. Solan, R. E. P. Winpenny, *Angew. Chem.* **1996**, *108*, 1967; *Angew. Chem. Int. Ed. Engl*. **1996**, *35*, 1825.
[13] A. Earnshaw, B. N. Figgis, J. Lewis, *J. Chem. Soc. A* **1966**, 1656; K. Nakata, A. Nagasawa, Y. Sasaki, T. Ito, *Chem. Lett*. **1989**, 753.
[14] J. A. Thich, B. H. Toby, D. A. Powers, J. A. Potenza, H. J. Schugar, *Inorg. Chem*. **1981**, *20*, 3314.
[15] T. Nakamoto, M. Hanaya, M. Katada, K. Endo, S. Kitagawa, H. Sano, *Inorg. Chem*. **1997**, *36*, 4347; C. E. Anson, J. P. Bourke, R. D. Cannon, U. A. Jayasooriya, M. Molinier, A. K. Powell, *Inorg. Chem*. **1997**, *36*, 1265; V. M. Lynch, J. W. Sibert, J. L. Sessler, B. E. Davis, *Acta Crystallogr. Sect. C* **1991**, *47*, 866.
[16] W. Micklitz, S. J. Lippard, *J. Am. Chem. Soc*. **1989**, *111*, 6856.
[17] K.-H. Kung, M. B. McBride, *Clays Clay Miner.* **1989**, *37*, 333.
[18] R. L. Parfitt, *Adv. Agronomy* **1978**, *30*, 1.
[19] A. E. Martell, L. G. Sillén, *Stability Constants of Metal–Ion Complexes*, Special Publication No. 25, The Chemical Society, London, **1971**.
[20] R. L. Parfitt, R. St. C. Smart, *J. Chem. Soc. Faraday Trans. 1* **1977**, *73*, 796; *Soil Sci. Soc. Am. J.* **1978**, *42*, 48.
[21] P. Agarwal, D. Landolt, *Corros. Sci.* **1998**, *40*, 673.
[22] S. Music, D. Dragcevic, S. Popovic, I. Czako-Nagy, *Croat. Chem. Acta* **1995**, *68*, 315.
[23] R. Docherty, K. J. Roberts, *Comp. Phys. Commun*. **1988**, *51*, 423, and references therein.
[24] S. Music, M. Gotic, S. Popovic, *J. Mater. Sci*. **1993**, *28*, 5744.
[25] A. Frini, M. El Maaoui, *J. Colloid Interface Sci.* **1997**, *190*, 269.
[26] A. Altomare, G. Cascarano, C. Giacovazzo, A. Guagliardi, *J. Appl. Crystallogr.* **1993**, *26*, 343.

Received: September 21, 1999 [F2036]